International Journal of the Physical Sciences Vol. 6(10), pp. 2507-2517, 18 May, 2011
Available online at http://www.academicjournals.org/IJPS
DOI: 10.5897/IJPS11.126
ISSN 1992 - 1950 ©2011 Academic Journals

Full Length Research Paper

Synthesis, spectral studies of 4-{[(3-substitutedphenyl)imino]methyl}-3-hydroxyphenyl octadecanoate and effect of *meta* substituents on mesomorphic properties

Sie-Tiong Ha[1]*, Yip-Foo Win[1], Siew-Ling Lee[2], Masato M. Ito[3], Kazuma Abe[3], Hidetoshi Oonishi[3] and Guan-Yeow Yeap[4]

[1]Department of Chemical Science, Faculty of Science, Universiti Tunku Abdul Rahman, Jln Universiti, Bandar Barat, 31900 Kampar, Perak, Malaysia.
[2]Ibnu Sina Institute for Fundamental Science Studies, Universiti Teknologi Malaysia, 81310 UTM Skudai, Johor, Malaysia.
[3]Faculty of Engineering, Soka University, 1-236 Tangi-cho, Hachioji, Tokyo 192-8577, Japan.
[4]Liquid Crystal Research Laboratory, School of Chemical Sciences, Universiti Sains Malaysia, 11800 Minden, Penang, Malaysia.

Accepted 20 April 2011

A series of Schiff base esters was synthesized from the reaction between 4-formyl-3-hydroxyphenyl octadecanoate and 3-substituted-anilines. The molecular structures were elucidated using spectroscopic techniques such as FT-IR and NMR. A conformational study associated with the presence of intramolecular hydrogen bonding which entails the formation of the keto-enol tautomerism in the solid and solution states are reported. Phase-transition temperatures and the thermal parameters were obtained from differential scanning calorimetry (DSC). The texture observation was carried out with a polarizing optical microscope (POM) over heating and cooling cycles. The title compounds exhibited direct isotropization process. The substituents at the *meta* position of the aniline fragment of benzylideneaniline compounds suppressed the formation of mesophase.

Key words: Schiff bases, 2D NMR, phase transition, mesophase.

INTRODUCTION

Mesomorphic behaviour of an organic compound is basically dependent on its molecular architecture, in which a slight change in the molecular geometry brings about considerable change in its mesomorphic properties. Detailed studies by liquid crystal researchers have led to empirical rules which include the effect of chemical constitution in the nematogenic and smectogenic mesophases (Gray, 1962). Numerous studies have been focused on Schiff's bases, ever since the discovery of 4-methoxybenzylidene-4'-butylaniline (MBBA) which exhibits a room temperature nematic phase (Kelker and Scheurle, 1969). Over the past few decades, low molecular weight Schiff's base esters have been investigated extensively. A lot of efforts have been made in order to generate its derivatives by introducing different substituents into the existing skeleton of the molecule. In these studies, the influence of a terminal alkyl chain upon the liquid crystalline properties (Ha et al., 2010a, b) and the possibility of enhancing the rigidity of the Schiff's base core system through metal complexes formation (Hoshino et al., 1998; Tian et al., 1996; Rao et al., 2002) have been claimed as favourable pathways to improve the mesogenic properties.

The presence of *ortho* hydroxyl group, for instance, has been regarded as one of the important elements which favours the existence of intramolecular hydrogen bonding (O-H···N and O···H-N) and also the tautomerism which

*Corresponding author. E-mail: hast_utar@yahoo.com, hast@utar.edu.my. Fax: +6054661676.

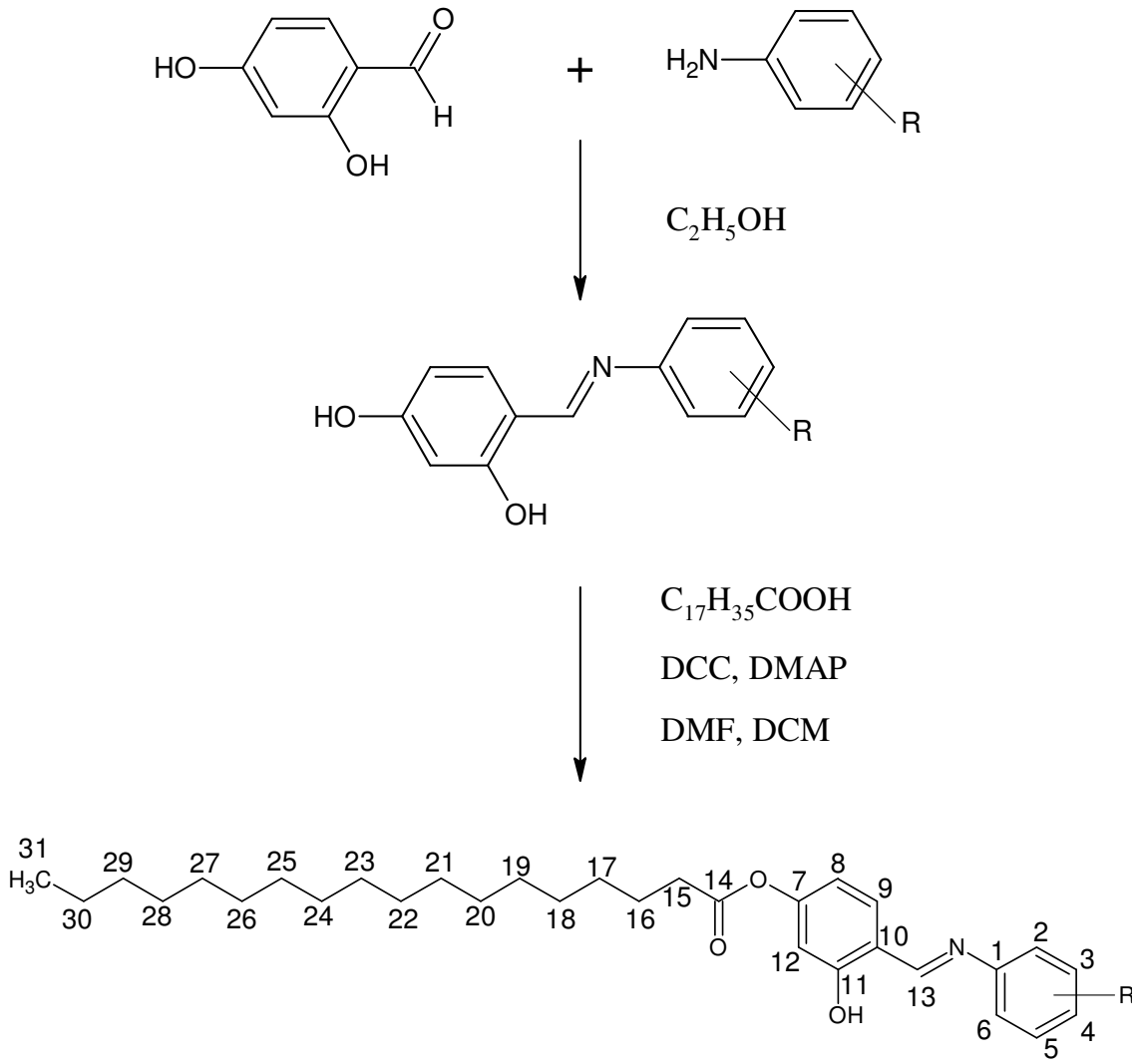

Figure 1. Synthetic and numbering scheme for Schiff bases SA-*m*-R and SA-*p*-R. SA-*m*-R; where R = H, Cl, CN, NO_2. SA-*p*-R, where R = Cl.

accounts for the formation of either enol-imino or keto-amino tautomer (Elmali et al., 1999). In order to explore further the factors which govern the thermal stability of liquid crystals with a Schiff's base core, and the structure-properties relationship, we carried out the investigation in a more comprehensive manner. More specifically, lateral substituents are placed at the *meta* position of the aniline fragment of benzylideneaniline compounds through preparation of 4-{[(3-substitutedphenyl)imino]methyl}-3-hydroxyphenyl octadecanoate (synthetic scheme is shown in Figure 1).

MATERIALS AND METHODS

Techniques

Electron impact mass spectra (EI-MS) were recorded by a Finnigan MAT95XL-T mass spectrometer operating at 70 eV ionizing energy. Microanalyses were carried out on Perkin Elmer 2400 LS Series CHNS/O analyser. FT-IR data were acquired on Perkin Elmer 2000-FTIR spectrophotometer in the frequency range of 4000 to 400 cm^{-1} with samples embedded in KBr discs. ^{1}H and ^{13}C NMR spectra were recorded in $CDCl_3$ by utilizing JEOL 400 MHz NMR Spectrometer with tetramethylsilane (TMS) as internal standard (at 400 and 100 MHz respectively). The phase transition temperatures were measured by Mettler Toledo DSC823 Differential Scanning Calorimeter (DSC) at a scanning rate of 10°C/min. Liquid crystalline properties were investigated by polarizing optical microscopy (POM) using a Carl Zeiss polarizing optical microscope (POM) attached to a Linkam Hotstage.

Materials

3-Aminobenzonitrile, 3-chloroaniline, 3-nitroaniline, aniline, 4-dimethylaminopyridine and stearic acid were obtained from Merck (Germany). Dicyclohexylcarbodiimide and 2,4-

Table 1. Infrared spectral data for SA-*m*-R.

Compound	*v* (O-H)	*v* (C-H aliphatic)	*v* (C=O of ester)	*v* (C=N)	*v* (C=C)	*v* (C-O)
SA-*m*-H	3445	2953, 2917, 2848	1757	1628	1596	1273
SA-*m*-Cl	3433	2952, 2917, 2848	1757	1625	1605	1273
SA-*m*-CN	3435	2954, 2916, 2852	1765	1619	1575	1270
SA-*m*-NO_2	3440	2952, 2916, 2851	1768	1626	1607	1272

dihydroxybenzaldehyde were obtained from Acros Organics (USA). All the reagents were used without further purification.

Synthesis of 3-hydroxy-4-[(phenylimino)methyl]phenyl octadecanoate (SA-*m*-H), 4-{[(3-chlorophenyl)imino]methyl}-3-hydroxyphenyl octadecanoate (SA-*m*-Cl), 4-{[(3-cyanophenyl)imino]methyl}-3-hydroxyphenyl octadecanoate (SA-*m*-CN) and 4-{[(3-nitrophenyl)imino]methyl}-3-hydroxyphenyl octadecanoate (SA-*m*-NO_2)

4-Formyl-3-hydroxyphenyl octadecanoate, was previously prepared via Steglich esterification (Ha et al., 2009). In a round-bottom flask, a mixture of the 4-formyl-3-hydroxyphenyl octadecanoate (5.0 mmol), 3-substituted aniline (5.0 mmol) and absolute ethanol (50 ml) was refluxed with stirring for 3 h. The reaction mixture was filtered and the residual solvent was removed from the filtrate by slow evaporation inside the fume hood. Recrystallization from absolute ethanol gave the title compounds as yellow solids (Yield: 51% for SA-*m*-H, 57% for SA-*m*-Cl, 41% for SA-*m*-CN, 13% for SA-*m*-NO_2).

RESULTS AND DISCUSSION

IR Spectroscopy

Absorption band assignable to the stretching of C=N bond for SA-*m*-Cl was observed at the frequency of 1625 cm^{-1} and this value conform with that reported in the IR spectra for various substituted aromatic Schiff bases which possesses a general formulation $HOC_6H_5CH{=}NC_6H_5$ (Yeap et al., 2002, 2004). A band assignable to the stretching of O-H bond is broadened at the frequency of 3433 cm^{-1} indicating the H atom from the O-H group in SA-*m*-Cl has a tendency to migrate to azomethine N atom via the O-H···N intramolecular hydrogen bonding as that observed for *meta* substituted 5-methoxysalicyaldimine isomer (Sal-*m*-R) in the solid state (Popovic, 2002).

Although the probable structure for SA-*m*-Cl have been postulated as enol-imino tautomer resembling Sal-*m*-R, further inspection upon the IR spectrum have disclosed that the stabilization of the enol-imino tautomer may vary depending on the type of *meta* substituent. This conformational study was based on the comparison of IR spectra of Schiff bases SA-*m*-R (where R = H, Cl, CN, NO_2) at different vibrational regions similar to the experimental observation reported for salicylideneaniline and naphthylidenequinolineamine (Unver, 2001; Salman and Salleh, 1997). A first comparison was made between the compound with free aniline fragment (SA-*m*-H) and the other compound in which the aniline was attached with a chlorine atom (SA-*m*-Cl). It is clearly shown from Table 1 that the C=N stretching band for SA-*m*-H occurs at a higher frequency, in comparison with that found for SA-*m*-Cl. This discrepancy can be rationalized by based on the electronegativity of chloro atom which can withdraw the electron density from the conjugated system involving the aromatic ring as well as the C=N bond.

As such, the strength of C=N bond in SA-*m*-Cl is weakened leading to the lowering of frequency. The presence of a very strong intensity of *v*(O-H) in compound SA-*m*-H further suggests that the azomethine C=N is not affected by H atom of O-H group via the intramolecular hydrogen bonding. This information also supports that the percentage of enol-imine in compound SA-*m*-H is comparatively higher than compound SA-*m*-Cl. Compounds SA-*m*-CN and SA-*m*-NO_2 show the similar characteristics as observed for compounds SA-*m*-H and SA-*m*-Cl. The stabilization of C=N bond which is accountable partially for the existence of enol-imino tautomer can also be inferred from the IR spectra of SA-*m*-CN and SA-*m*-NO_2. However, it is suggested that the π-electron density from CN substituent would increase the stability of the keto-amino instead of enol-imino tautomer, due to the increase of the basicity of the azomethine nitrogen. The significant difference of C=C aromatic frequency between SA-*m*-CN and SA-*m*-NO_2 also indicates that the percentage of enol-imine in SA-*m*-NO_2 is comparatively higher than that in SA-*m*-CN.

NMR Spectroscopy

The molecular structure of the title compounds (Figure 1) is furthered ascertained using NMR techniques. The chemical shifts of each atom (proton and carbon) in the molecular structure of SA-*m*-R (where R = H, Cl, CN, NO_2) are obtained by means of ^1H-^1H and ^{13}C-^1H correlation spectroscopic measurements and tabulated in Tables 2 and 3. The ^1H-^1H and ^{13}C-^1H relationships of the title compounds is shown in Tables 4 and 5, respectively. The 2D COSY, 2D HMQC and 2D HMBC spectra of SA-*m*-Cl are shown as representative illustration in Figures 2 to 4, respectively. Two triplets at δ = 0.91 ppm and δ = 2.58 ppm in the ^1H NMR spectrum, can either be due to the H31 or H15 atoms because only both of these atoms

Table 2. ^{1}H NMR chemical shifts of SA-*m*-R in $CDCl_3$.

Compounds	Chemical shifts (ppm)													
	H2	H3	H4	H6	H8	H9	H12	H13	OH	H15	H16	H17-H30	H31	H5
SA-*m*-H	7.45 (m)[b]	7.31 (m)[c]	7.29 (m)	7.45 (m)[b]	6.71 (dd) *J* = 2.2, 8.4 Hz	7.40-7.42 (d) *J* = 8.4 Hz	6.79 (d) *J* = 2.2 Hz	8.63 (s)	13.59 (s)	2.59 (t)	1.78 (quint)	1.28-1.46 (m)	0.91 (t)	7.31 (m)[c]
SA-*m*-Cl	7.17 (m)	7.35 (d)	7.27 (m)[d]	7.28 (d)[d]	6.73 (dd) *J* = 2.2, 8.4 Hz	7.40 (d) *J* = 8.5 Hz	6.79 (d) *J* = 2.2 Hz	8.58 (s)	13.20 (s)	2.58 (t)	1.78 (quint)	1.29-1.45 (m)	0.91 (t)	-
SA-*m*-CN	7.58 (m)	7.49 (dt)	7.53 (m)[d]	7.54 (d)[d]	6.74 (dd) *J* = 2.2, 8.4 Hz	7.41 (d) *J* = 8.4 Hz	6.79 (d) *J* = 2.2 Hz	8.59 (s)	12.92 (s)	2.58 (t)	1.77 (quint)	1.28-1.43 (m)	0.90 (t)	-
SA-*m*-NO_2	8.14 (m)	8.16 (m)	7.61 (d)[d]	7.60 (d)[d]	6.76 (dd) *J* = 2.0, 8.4 Hz	7.44 (d) *J* = 8.4 Hz	6.80 (d) *J* = 2.0 Hz	8.67 (s)	12.91 (s)	2.59 (t)	1.78 (quint)	1.28-1.44 (m)	0.90 (t)	-

s = singlet, d = doublet, dd = double doublets, t = triplet, dt = doublet triplets, quint = quintet, m = multiplet, [a] TMS used as internal standard. [b] H2 and H6 are equivalent protons. [c] H3 and H5 are equivalent protons. [d] The signals attributed to H4 and H6 protons are overlapping each other.

(H31 and H15) possess two adjacent hydrogens which will give a triplet signal in the ^{1}H NMR spectrum.

It can be resolved by HMBC experiment (Figure 4 and Table 5) wherein a cross peak observed between carbonyl carbon C14 with a ^{1}H signal at δ = 2.58 ppm and confirmed that this ^{1}H signal belonged to H15 atom because C14 atom is very near to H15 atom compared to H31 atom (Figure 1). The other triplet at δ = 0.91 ppm is attributed to the H31 atom and was supported by the integrated ^{1}H signals showing a total of three hydrogens. A quintet signal which appeared at δ = 1.78 ppm is attributed to one of the methylene protons at C16 to C30 but its actual position cannot be determined in the normal ^{1}H NMR spectrum. Further investigation via COSY experiment revealed that this quintet signal was attributed to H16 atom because H16 atom correlated with both adjacent hydrogens (H15 and H17) in the COSY spectrum (Table 4). The doublet signals observed at δ = 6.79 ppm (*J* = 2.17 Hz) and δ = 7.40 ppm (*J* = 8.48 Hz) are attributed to H12 and H9 atoms, respectively. This ^{1}H NMR assignment was obtained based on the theory (Landgrebe, 1993) that a proton (H8) coupled with a proton (H12) which is *meta* to its position will give smaller coupling constants (*J* = 2.17 Hz), while the proton (H8) coupled with a proton (H9) which is *ortho* to its position will result in higher coupling constants (*J* = 8.48 Hz). The homonuclear connectivity between H8 proton with H9 proton which is *ortho* to its position and H12 proton which is *meta* to its position (Table 4) gave rise to a double of doublets signals at δ = 6.73 ppm which is attributed to atom H8.

The ^{13}C spectral assignment (Table 3) was obtained by studying the ^{13}C, DEPT, ^{13}C-^{1}H HMQC and HMBC experiments. Assignments of 1°, 2° and 3° carbons was made by 2D (^{13}C-^{1}H HMQC) experiment using delay values which corresponds to ^{1}J(C,H). The HMQC spectra of SA-*m*-Cl revealed that the signal at δ = 14.53 ppm contained resonance position for methyl carbon, which was attributed to C31 due to the cross peak with H31 at δ = 0.91 ppm. In addition, atom H16 was correlated with atom C16 at δ = 25.29 ppm and atom H15 correlated with C15 at δ = 34.84 ppm. HMQC spectrum also revealed the attachments between aromatic hydrogens and their corresponding carbons. From the plot (Figure 3), we can clearly assign C2 at δ = 120.12 ppm, C3 at δ = 130.82 ppm, C4 at δ = 127.26 ppm and C6 at δ = 121.62 ppm. HMQC spectrum also showed the cross peak of H8 proton with C8 carbon at δ = 113.50 ppm, H9 proton with C9 carbon at δ = 133.82 ppm and H12 proton with C12 carbon at δ = 110.91 ppm. Finally, the azomethine carbon, C13 at δ = 163.18 ppm was assigned based on the cross peak with azomethine proton, H13 at δ = 8.58 ppm.

The quaternary carbons were established throughout the connectivities between the protonated carbons fragment by using long range correlated HMBC experiment (Table 5 and Figure 4a). Thus, the long range HMBC cross peaks of

Table 3. ^{13}C NMR chemical shifts SA-*m*-R in $CDCl_3$.

Atom C	Chemical Shifts (ppm)			
	SA-*m*-H	**SA-*m*-Cl**	**SA-*m*-CN**	**SA-*m*-NO_2**
C1	148.64	150.00	149.62	149.98
C2	121.55[a]	120.12	126.36	128.35
C3	129.83[b]	130.82	130.53[d]	130.68
C4	122.37	127.26	130.53[d]	121.76
C5	129.83[b]	135.50	113.99	149.50
C6	121.55[a]	121.62	124.89	116.01
C7	154.91	155.28	155.63	155.72
C8	113.27	113.50	113.74	113.80
C9	133.51	133.82	134.12	134.21
C10	117.53	117.25	117.05	117.01
C11	162.96	162.92	162.91	162.95
C12	110.86	110.91	110.98	111.00
C13	162.16	163.18	164.23	164.59
C14	172.13	172.04	172.00	172.00
C15	34.86	34.84	34.82	34.83
C16	25.29	25.29	25.26	25.26
C17-C28[c]	29.49, 29.65, 29.77, 29.86, 30.00, 30.02, 30.05, 30.07, 30.10, 30.12, 30.15	29.49, 29.67, 29.78, 29.88, 30.02, 30.07, 30.08, 30.10, 30.12	29.48, 29.65, 29.77, 29.86, 30.01, 30.03, 30.06, 30.09, 30.11, 30.14	29.48, 29.66, 29.76, 29.86, 30.00, 30.02. 30.05, 30.07, 30.09 30.10, 30.12, 30.15
C29	32.33	32.34	32.33	32.33
C30	23.09	23.11	23.09	23.09
C31	14.52	14.53	14.52	14.51
CN	-	-	118.59	-

TMS used as internal standard. [a]C2 and C6 are equivalent carbons. [b]C3 and C5 are equivalent carbons. [c]Some of the signals attributed to C17-C28 (D) appear in the same column in the ^{13}C NMR spectra which resulted in less than 12 signals observed in the ^{13}C NMR spectra. [d]Overlapped.

H13 with C1 at δ = 150.00 ppm, H4 and H6 with C5 at δ = 135.50 ppm, H8 and H9 with C7 at δ = 155.28 ppm support firmly the position of these atoms. Atom C10 at δ = 117.25 ppm in the ^{13}C NMR spectra is assigned based on the correlation with its nearest neighbour H13 atom in the HMBC spectra. The ^{13}C signal of C11 atom at δ = 162.92 ppm was confirmed via correlation between the hydroxyl proton and C11 atom in the HMBC experiment (Figure 4a). While, the carbonyl carbon, C14 appeared at δ = 172.04 ppm was assigned based on the heteronuclear connectivities with the methylene protons, H15 at δ = 2.58 ppm and H16 at δ = 1.78 ppm (Table 5).

SA-*m*-Cl shows two singlet peaks at δ = 8.58 and 13.20 ppm which can be attributed to CH=N and OH, respectively. The singlet attributed to the azomethine proton indicates the absence of a proton at the nitrogen atom and the absence of CH-NH coupling (Nazir et al., 2000). This phenomenon has further been supported by NMR technique as that reported by Alarcon et al. (1994) wherein the *ortho* hydroxy group attached to the aldehyde ring in $HOC_6H_5CH{=}NC_6H_5$ exists as an enol-imino tautomer when left standing in the solution ($CDCl_3$). The tautomerism of the title compound is further investigated by ^{13}C NMR spectroscopy. The most

Table 4. ^{1}H-^{1}H COSY correlations of SA-*m*-Cl in $CDCl_3$.

Atom H	^{1}H-^{1}H COSY correlations
2	3, 4, 6
3	2, 4
4	2, 3, 6
6	2, 4, 13
8	9, 12
9	8, 13
12	8
13	6, 9
OH	-
15	16
16	15
H17-H30	16, 31
H31	H17-H30

Table 5. 2D ^{1}H-^{13}C HMQC and HMBC correlations of SA-*m*-Cl in $CDCl_3$.

Atom	HMQC	HMBC [*J*(C,H)]			
	^{1}J	^{2}J	^{3}J	^{4}J	^{a}J
H2	C2	C3	C4, C6	-	-
H3	C3	C2, C4	-	-	C13
H4	C4	C5	C2	-	-
H6	C6	C1, C5	C2, C4	-	-
H8	C8	C7	C10	-	-
H9	C9	-	C7	-	-
H12	C12	C7, C11	C8, C10	-	-
H13	C13	C10	C1, C9, C11	C12	-
OH	-	C11	C10, C12	C7, C13	-
H15[b]	C15	C16, C14	-	-	-
H16[b]	C16	C15	C14	-	-
H17-H28	C17-C28	-	-	-	-
H31[b]	C31	C30	C29	-	-

[a]Intramolecular interaction; [b]Correlate with methylene carbons in the alkyl chain (C17-C28) but cannot determine their real positions because ^{13}C chemical shifts for the methylene chain cannot be distinguished.

tautomerization-sensitive signals belonging to C11 and C13 located in the range of δ = 162-164 ppm, indicating that the proton is bonded to the OH group. This seems to suggest that the keto-enol equilibrium is in favour of enol in $CDCl_3$ solution. The ^{13}C NMR data obtained are in accordance with the information for N-(2-hydroxybenzylidene)anilines as reported by Zheglova et al. (1995).

Similar characteristics shown by SA-*m*-H, SA-*m*-CN, SA-*m*-NO_2 are also favourable for the assignments of H and C atoms (Tables 2 and 3). In-depth study on ^{1}H-^{1}H and ^{13}C-^{1}H interactions of SA-*m*-Cl was carried out in order to postulate the possible conformation in the solution ($CDCl_3$). The ^{1}H-^{1}H and ^{13}C-^{1}H relationships as observed between atoms (C and H) in the aldehyde and aniline fragments is tabulated in Tables 4 and 5. Inspection from COSY (Table 4 and Figure 2) and HMBC (Table 5 and Figure 4a) can be summarized as follows:

(a) By 2D COSY experiment, H13 proton was found to be correlated with H9 proton.
(b) In the HMBC experiment, H13 proton was found to be correlated with C1, C9 and C10 carbons.
(c) No ^{1}H-^{1}H connectivities was observed between H13 and hydroxyl (O-H) protons in the 2D COSY experiment.
(d) The summary (a) to (b) suggests that H13 proton was located nearer to atoms at the position 1, 9 and 10 (Figure 1) rather than hydroxyl proton owing to none interaction between H13 and hydroxyl protons in summary as those discussed in (c).

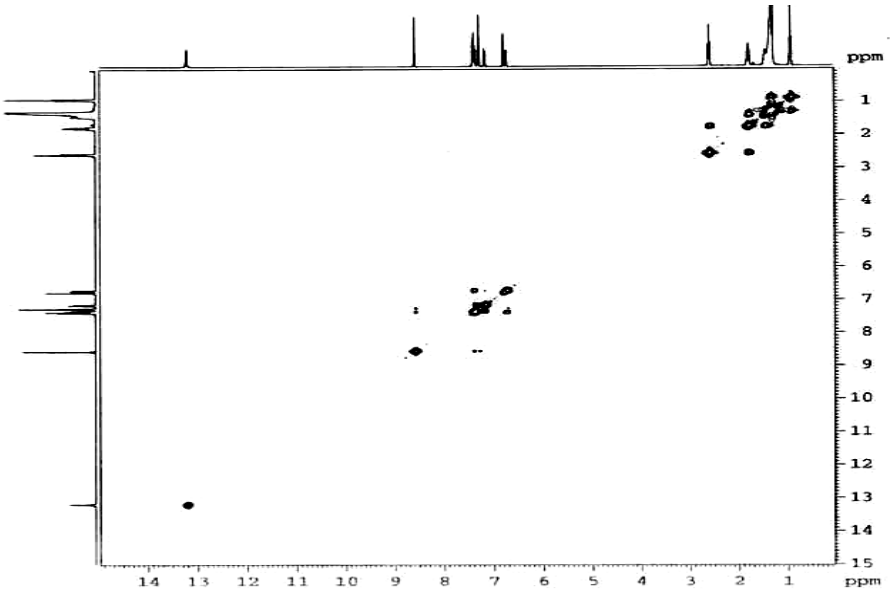

Figure 2. ^{1}H-^{1}H COSY spectrum of Schiff base SA-*m*-Cl.

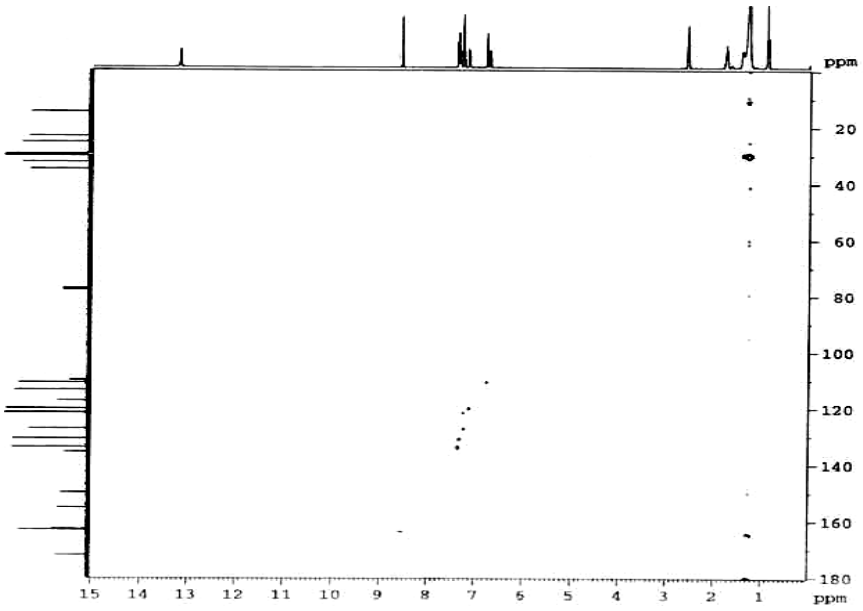

Figure 3. ^{13}C -^{1}H HMQC spectrum of Schiff base SA-*m*-Cl.

(e) The hydroxyl proton was found to be correlated with carbons in the aldehyde fragment, C7, C10, C11 and C12 carbons in the HMBC experiment.

(f) The hydroxyl proton was found not to be correlated with atom C8, C9 and carbons in the aniline fragment (C1, C2, C3, C4, C5 and C6) in the HMBC experiment.

The summary from (a) to (e) suggests that the azomethine proton (H13) was located at the other side opposing to the OH group. As such, the distance between hydroxyl proton (O-H) and the azomethine proton (H13) increases and, subsequently, no ^{1}H-^{1}H correlation between them will be observed in the 2D COSY spectrum. The probable conformation of SA-*m*-Cl can be best represented in Figure 4b. As discussed in (e) to (f), the hydroxyl proton was found to be correlated with the carbons in the aldehyde fragment (C7, C10, C11 and C12) but not correlated with the carbons in the aniline fragment which indicated that the *cis-trans* isomerism of SA-*m*-Cl is in favour of trans configuration. The *trans* isomer of SA-*m*-Cl is depicted in Figure 4b. The *cis*

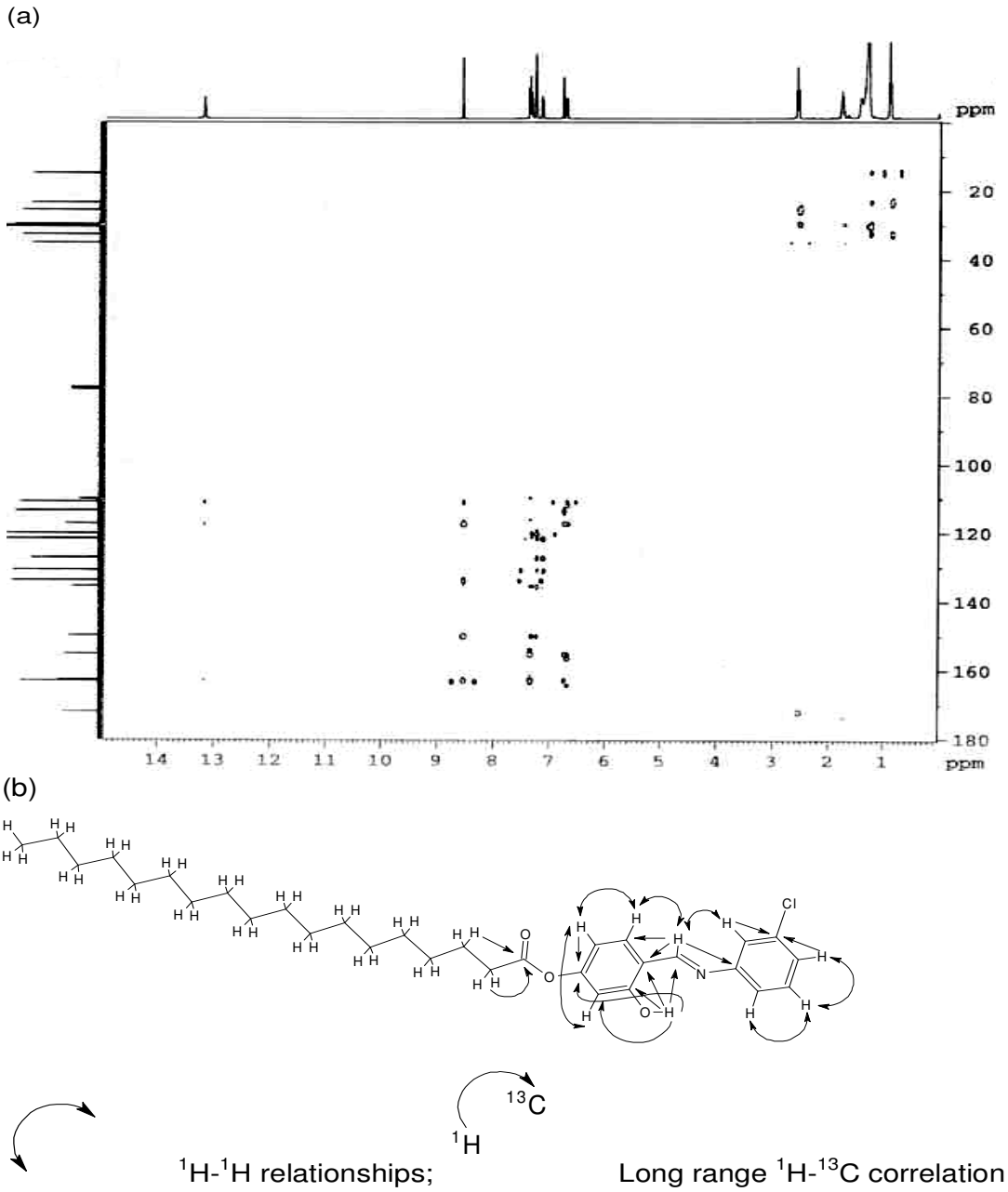

Figure 4. (a) Heteronuclear 2D ^{13}C -^{1}H HMBC spectrum, (b) ^{13}C-^{1}H long range connectivites and preferred conformation as inferred from 2D HMBC spectra of Schiff base SA-*m*-Cl. The preferred conformation is supported by ^{1}H-^{1}H relationships obtained from 2D COSY spectra.

configuration may be possible only if the ^{13}C-^{1}H connectivities are observed between the hydroxyl proton and carbons in the aniline fragment because in the *cis* configuration, the hydroxyl proton is in close proximity with carbons in the aniline fragment.

Although the probable structure has been postulated as a *trans* isomer, as depicted in Figure 4b, but the real position of the atom chlorine in the aniline fragment still remained ambiguous. It is because the rotation of the aniline fragment at C10-C13-N-C1 torsion angle will give different types of configurations. The first type configuration can be referred to as the location of atom chlorine in the aniline fragment at the same side with hydroxy (O-H) group as shown in Figure 1. The rotation of the aniline fragment from its actual position in Figure 1 until the atom chlorine was located at the other side will give rise to the second type configuration (Figure 4b). By 2D COSY experiment (Table 4), H13 proton was found to be correlated with H6 proton but not with H2 proton. This piece of information seems to suggest that the H13

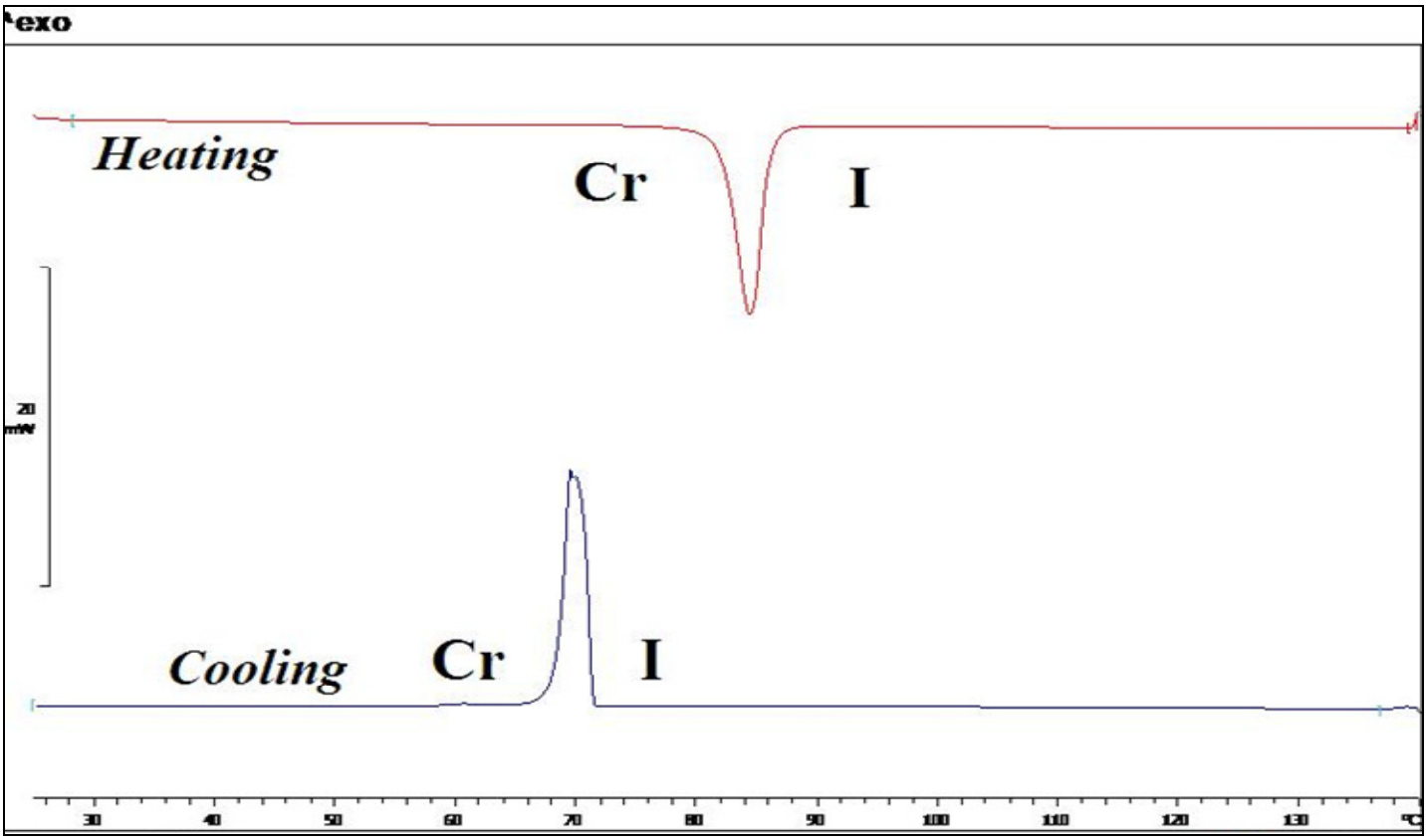

(a)

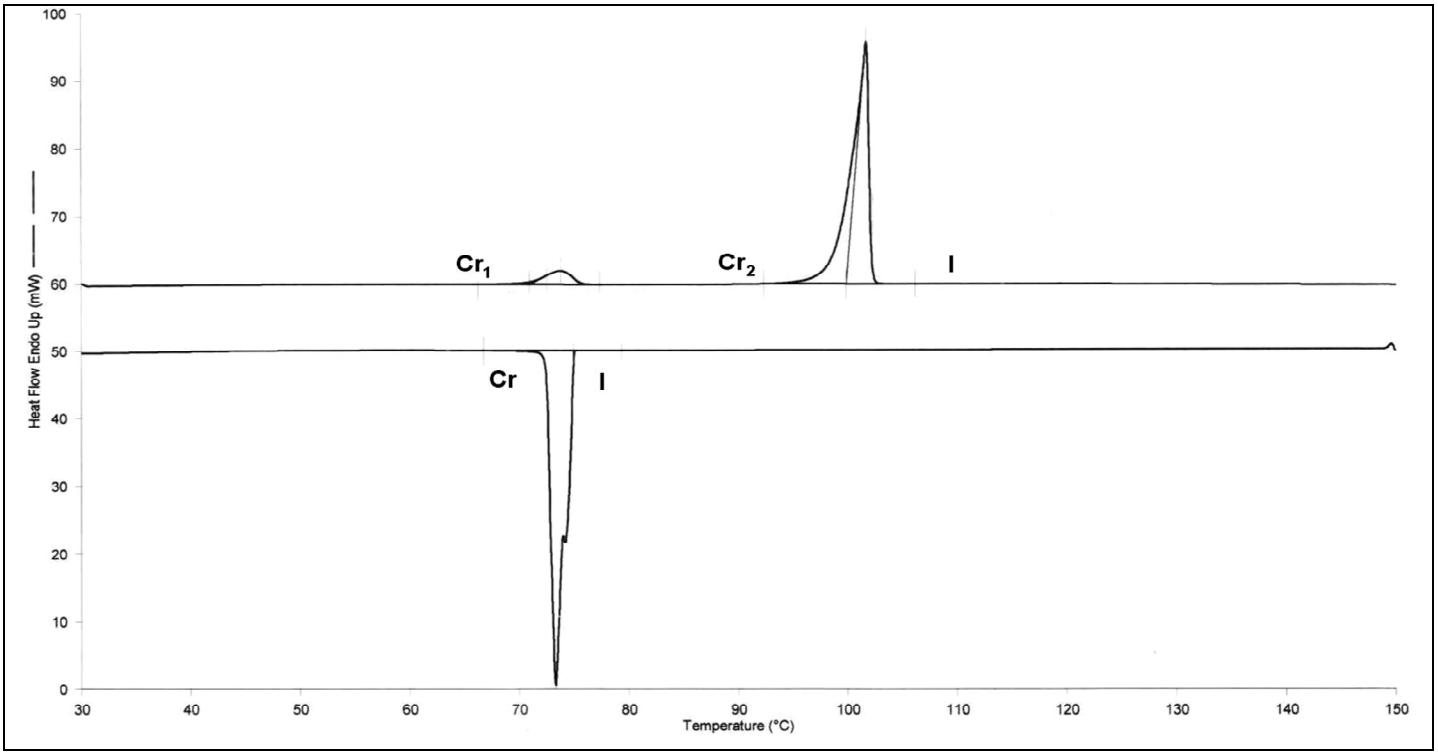

(b)

Figure 5. DSC thermogram of (a) SA-*m*-H and (b) SA-*m*-Cl upon heating and cooling cycles.

Table 6. Transition temperature and associated enthalpy changes of SA-*m*-H, SA-*m*-Cl, SA-*m*-CN, SA-*m*-NO_2 and SA-*p*-Cl upon heating and cooling.

Compound	Transition temperature, ℃ (ΔH, kJ mol^{-1})	
	Heating	Cooling
SA-*m*-H	Cr 84.5 (83.2) I	Cr 70.0 (84.3) I
SA-*m*-Cl	Cr_1 73.7 (6.8) Cr_2 101.7 (74.7) I	Cr 73.3 (76.9) I
SA-*m*-CN	Cr 94.8 (73.4) I	Cr 77.3 (71.7) I
SA-*m*-NO_2	Cr 110.1* I	Cr 97.3* I
SA-*p*-Cl	Cr_1 94.8 (12.3) Cr_2 116.1 (65.9) SmA 123.8 (10.2) I	Cr_1 78.6 (11.2) Cr_2 104.8 (68.9) SmA 119.8 (10.6) I

Cr, crystal; SmA, Smectic A; I, isotropic, *polarizing optical microscopy data.

proton was located nearer to H6 proton rather than H2 proton and can be best represented in Figure 4b, whereby the real position of atom chlorine was determined.

Phase transition behaviors, optical texture studies and effect of *meta*-substituent on mesomorphic properties

The phase transition temperatures and their associated enthalpy obtained from DSC analysis over heating and cooling cycles are tabulated in Table 6. DSC thermogram of SA-*m*-Cl (Figure 5b) showed an endotherm at 73.73℃ before isotropization. The texture observed under the polarizing microscope is indicative of the presence of subphases within the crystal phase (Cr_1-Cr_2) as those observed in its analogue *o*-*n*-hydroxy-*p*-*n*-hexadecanoyloxybenzylidene-fluoroaniline (Yeap et al., 2004). The change of chloro position at *meta*-position in SA-*m*-Cl to *para*-position in SA-*p*-Cl has drastically influenced the mesomorphic properties. SA-*m*-Cl is non-mesogenic. Even the supercooling of these compounds failed to produce a monotropic mesophase. These results indicate that chloro substituent at the *meta*-position is unfavourable for the formation of mesophases, in contrast to SA-*p*-Cl with the chloro substituent at the *para*-position.

One of the probable reasons is that the chloro substituent at the *meta*-position, exerts a molecular broadening influence, reducing the lateral intermolecular force of attraction and thus impeding liquid crystal formation (Sakagami, 2001). Furthermore, SA-*m*-Cl possessed lower melting point compared to SA-*p*-Cl having the similar number of carbons (n) at the alkanoyloxy chain. This suggests that the substitution at the *meta*-position can depress the thermal stability of a compound. In the representative DSC thermogram of SA-*m*-H (Figure 5a), it showed an endotherm and exotherm, respectively during both heating and cooling cycles. This observation indicates direct melting of the crystal phase to the isotropic liquid phase and vice versa. Under polarizing optical microscopy (POM) observation, crystal changed to dark region isotropic during heating run. No liquid crystal texture was observed during cooling process. Other derivatives, SA-*m*-CN, SA-*m*-NO_2 showed the similar characteristics as those found for SA-*m*-H.

ACKNOWLEGDEMENTS

The authors would like to thank Universiti Tunku Abdul Rahman (UTAR) for UTAR Research Fund and the Ministry of Higher Education (MOHE) for the financial support.

REFERENCES

Alarcon SH, Olivieri AC, Gonzalez-Sierra M (1994). ^{13}C NMR Spectroscopic and AM1 Study of The Intramolecular Proton Transfer in Anils of Salicyaldehyde and 2-Hydroxynaphthalene-1-carbaldehyde. J. Chem. Soc. Perkin Trans., 2: 1067-1070.

Elmali A, Kabak M, Kavlakoglu E, Elerman Y, Durlu TN (1999). Tautomeric Properties, Conformation and Structure of *N*-(2-hydroxy-5-chlorophenyl) Salicyaldimine. J. Mol. Struct., 510: 207-214.

Gray GW (1962). Molecular structure and properties of liquid crystals. Academic Press, London.

Ha ST, Ong LK, Sivasothy Y, Yeap GY, Boey PL, Lin HC (2010a). New mesogenic Schiff base esters with polar chloro substituent: Synthesis, thermotropic properties and x-ray diffraction studies. Am. J. Appl. Sci., 7(2): 214-220.

Ha ST, Ong LK, Sivasothy Y, Yeap GY, Lin HC, Lee SL, Boey PL, Bonde NL (2010b). Mesogenic Schiff base esters with terminal chloro group: Synthesis, thermotropic properties and X-ray diffraction studies. Int. J. Phys. Sci., 5: 564-575.

Ha ST, Ong ST, Chong YT, Yeap GY (2009). Synthesis of 4-{[(3-chlorophenyl)imino]methyl}-3-hydroxyphenyl myristate. Molbank, 4: M629.

Hoshino N, Takashi K, Sekiuchi T, Tanaka H, Matsunaga Y (1998). Smectogenic Copper(II) complexes of N-salicylideneaniline derivatives. A comparative study of homologous series carrying alkoxy and/or alkanoyloxy substituents. Inorg. Chem., 37: 882-889.

Kelker H, Scheurle B (1969). A liquid crystalline (nematic) phase with a particularly low solidification point. Angew. Chem. Int. Edn., 8: 884–885.

Landgrebe JA (1993). Theory and Practice in the Organic Laboratory, Brooks/Cole Publishing Company, California.

Nazir H, Yildiz M, Yilmaz H, Tahir MN, Ulku D (2000). Intramolecular Hydrogen Bonding and Tautomerism in Schiff Bases. Structure of *N*-2-(2-pyridil)-2-oxo-1-napthylidenemethylamine). J. Mol. Struct., 524: 241-250.

Popovic Z, Pavlovic G, Calogovic DM, Rohe V, Leban L (2002). On Tautomerism of Two 5-Methoxysalicyaldimine Structural Isomers in

the Solid State: Structural Study *N*-(*o*-hydroxyphenyl)-5-methoxysalicyaldimine and *N*-(*m*-hydroxyphenyl)-5-methoxysalicyaldimine. J. Mol. Struct., 615: 23-31.
Rao NVS, Singha D, Das M, Paul MK (2002). Synthesis and mesomorphic properties of *N*(4-*n*-alkyloxy salicylidene) 4'-n-alkylanilines and their copper complexes. Mol. Cryst. Liq. Cryst., 373: 105-117.
Sakagami S, Koga T, Nakamizo M, Takase A (2001). Spectroscopic study of liquid crystalline N-[4-(4-n-alkoxybenzoyloxy)-2-hydroxybenzylidene]hydroxyanilines. Liq. Cryst., 28: 347-350.
Salman SR, Salleh NAI (1997). Infra-red Study of Tautomerism in Some Schiff Bases. Spectrosc. Lett., 30(7): 1289.
Tian Y, Su F, Xing P, Zhao Y, Tang X, Zhao X, Zhou E (1996). Synthesis of a new series of chiral Schiff's bases and their copper complexes. Liq. Cryst., 20: 139-145.
Unver H (2001). Synthesis and Spectroscopic Studies in Some New Schiff Bases. Spectrosc. Lett., 34(6): 783-791.
Yeap GY, Ha ST, Lim PL, Boey PL, Mahmood WAK, Ito MM, Sanehisa S (2004). Synthesis and mesomorphic properties of Schiff base esters ortho-hydroxy-para-alkyloxybenzylidene-para-substituted anilines. Mol. Cryst. Liq. Cryst., 423: 73-84.
Yeap GY, Ooi WS, Nakamura Y, Cheng Z (2002). Synthesis and mesomorphic properties of Schiff base esters *p*-*n*-octadecanoyloxy-benzylidene-*p*-cyano-, *p*-hydroxy-, *p*-nitro- and *p*-carboxyanilines. Mol. Cryst. Liq. Cryst., 381: 169-178.
Zhegolva DK, Gindin V, Kol'tsov AI (1995). Tautomerism of N-(2-Hydroxybenzylidene) anilines in The Crystalline State and in Solution Studied by Nuclear Magnetic Resonance Specroscopy. J. Chem. Res., 32.